

LYMPHATIC ARCHITECTURE OF SUNCUS MURINUS (HOUSE MUSK SHREW) PALATUM

S. Hatakeyama, Y. Ando, H. Miura, K. Satoh, A. Fujimura

Departments of Oral Health Enhancement, Division of Orthodontics (SH,KS) and General Dentistry, Division of General Dentistry Education (HM), School of Dentistry; and Department of Anatomy (YA,AF), Division of Functional Morphology, Iwate Medical University, Japan

ABSTRACT

The architecture of craniocervical lymphatic vessels in rodents has been examined previously. In the present study, we evaluated the distribution of collecting lymphatic vessels in the palate of Suncus, which is known to retain the prototype of placental mammals and is more similar to humans in terms of jaw bone morphology when compared with rodents.

Three-dimensional reconstructed images of the Suncus palatum revealed that the collecting lymphatic vessels were connected to each other via smaller branches, and ran in an antero-posterior direction in the periosteum. The vessels entered the pair of posterior palatine foramina located near the fourth premolar or the first molar bilaterally, coursed through the posterior palatine canals, and reached the pterygopalatine fossa positioned posteriorly in the palate. The collecting lymphatic vessels changed directions from medial to superior to lateral while wrapping around arteries during their course, perhaps to enable the smooth transition from the palate to the deep cervical node. Inefficient lymphatic flow in humans is attributed to the superior location of the pterygopalatine fossa in the palate when compared with its location in the Suncus.

Keywords: *Sucus murinus*, shrew,

craniocervical lymphatic architecture, palate, dentition, 5'-nucleotidase

Detailed investigations of the lymphatic distribution in the oral cavity are lacking. In humans, it is known that the palate is the only part of the oral cavity where lymphatic vessels drain directly into the deep cervical nodes without passing through the submandibular nodes. However, there are no reports regarding the routes of these vessels mid-course. Although architecture of peripheral lymphatic capillaries in the palate has been reported previously (1), no studies on collecting lymphatic vessels have been conducted.

Our group has been investigating the architecture of the craniocervical lymphatic vessels in rodents (2-11). It is obvious that the oral cavity of mice cannot be used to simulate the collecting lymphatic vessels of the palate in humans, mainly due to the difference in the number of teeth. The dentition of mice differs greatly from that of humans, and is characterized by rootless incisors and edentulous areas due to missing canines and premolars. Additionally, the mouse palate consists of a large incisive fossa that connects to the nasal cavity. Moreover, masticatory movement in mice is based on the antero-posterior shift of the mandible and accounts for the morphological differences in the oral cavity between mice and humans. Recently,

the Suncus is drawing attention due to its potential for use as a small experimental animal in the field of dentistry. The dentition of this animal is described as I3/1C1/1P2/1M3/3 = 30 and all teeth have roots. Based on these factors, we used the Suncus to investigate the architecture of collecting lymphatic vessels, in the present study.

MATERIALS AND METHODS

Experimental Animals

Ten Suncus (4-week-old; male; approximately 50 g; NAG) were used in this study. They were donated by Professor Sen-ichi Oda and Lecturer Takamichi Jogahara of Okayama University of Science, College of Science, Department of Zoology, Okayama, Japan, and housed at the Institute for Experimental Animal Sciences Iwate Medical University Iwate, Japan (air temperature: 26°C, humidity: 55.0%). The animals had free access to trout feed pellets (Japan Clea) and water. This study was approved by the Committee of Animal Experiments, Iwate Medical University (Approval number 22-024) and all experiments were conducted in accordance with the guidelines for animal experiments at Iwate Medical University based on "Guidelines for Proper Conduct of Animal Experiments" from the Ministry of Education, Culture, Sports, Science and Technology in Japan.

Investigation of the Structure of the Palate

Micro-CT imaging

The Suncus were sacrificed by CO₂ inhalation after which the heads were sectioned. Serial topographic images (tube voltage, 80kV; tube current, 450 μA; 512x512 pixels; thickness, 27 μm) using Micro-CT (RS80®, GE Healthcare, USA) were obtained. Subsequently, three-dimensionally reconstructed images were developed using software (ZedView, Ver.9.3, LEXI, Japan). Multi Planar Reconstruction (MPR) images

obtained from the three-dimensional images were used for the observation of the architecture of the vessels in the hard palate.

Hematoxylin Eosin (H-E) staining

After sacrificing the Suncus by CO₂ inhalation the heads were sectioned and the outer surface of the skin was removed. Thereafter, the samples were fixed in 10% formalin for one week at room temperature followed by decalcification for two weeks at room temperature using Plank-Rychlo's solution. The samples were dehydrated in an ascending series of alcohol, placed in xylene, and subsequently embedded in paraffin. Sagittal and frontal serial sections (10 μm) were fabricated using a sliding microtome, and H-E staining was performed prior to embedding. The two-dimensional histological structures of the hard and soft palates were observed using a light microscope (VHX-1000®, KEYENCE, Japan) by merging the images.

Staining of lymphatic vessels and three-dimensional reconstruction

A segment of the palate including surrounding hard and soft tissues was removed from the sacrificed Suncus and all teeth were extracted. The non-decalcified samples were cryo-embedded in 5% carboxymethyl cellulose (CMC) in hexane cooled with liquid nitrogen. Thereafter, the specimens were placed in a cryostat (CM3050S®, Leica, Germany) with blade angles of 5°, OT: -22°, and CT: -23°, and serial, non-decalcified, frontal sections (10 μm) were produced using the film-transfer method as described previously (12). After washing the sections with tris-maleate buffer solution, they were immersed in 5'-nucleotidase substrate solution (5'-Nase) for 40 minutes at 37°C in order to identify the lymphatic vessels (3,13). The substrate solution consisted of 25 mg of 5'-adenosine monophosphate, 5 ml of 0.1M MgSO₄, 3 ml of 2% Pb(NO₃)₂,

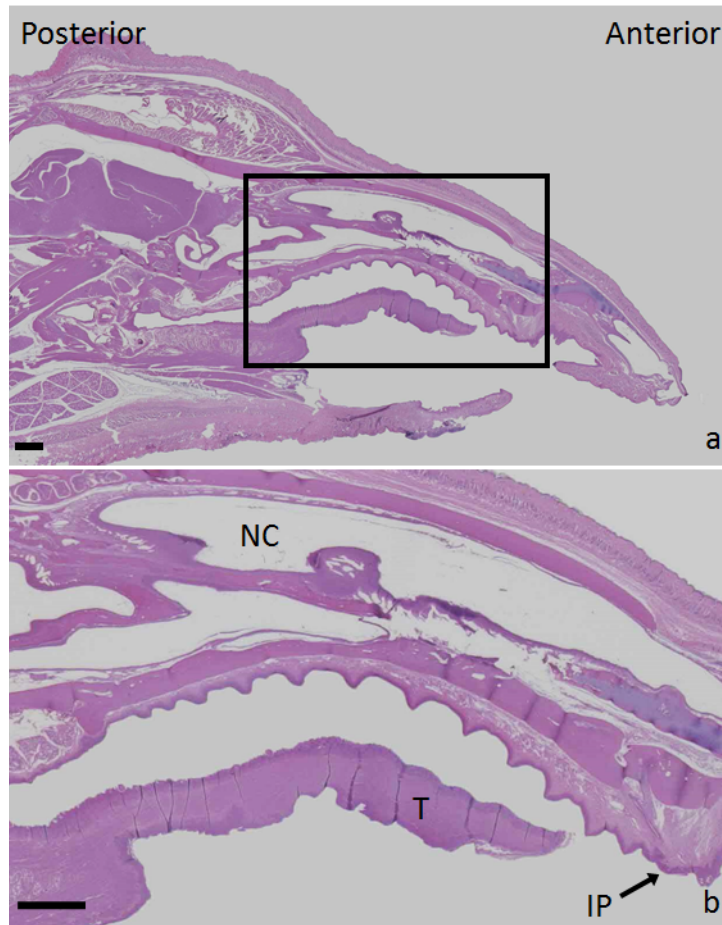


Fig. 1. H-E stained images of the head. a) sagittal section. b) Magnified image of the square in Fig. 1a. There were 12 transverse palatine folds posterior to the incisive papilla. Thickness of mucosal tissue becomes thinner as you trace to the posterior region. NC: nasal cavity, T: tongue, IP: incisive papilla, (bar: 1000 μ m)

20 mg of levamisole, 20 ml of 0.2M tris-maleate buffer solution and 22 ml of distilled water. After rinsing again with tris-maleate buffer solution, the sections were immersed in 1% ammonium sulfide solution for 2 min at room temperature for coloring of lymphatic vessels. Then, after washing with distilled water, the sections were embedded in 30% glycerin and observed under a light microscope. The dark brown colored lymphatic vessels were detected by observing the captured two-dimensional images on the monitor. Coordination of the axes and threshold image processing (Photoshop®CC, Ver.14.0, Adobe, USA) was performed to

observe the distribution of the lymphatic vessels using the aforementioned three-dimensional reconstruction software (13,14).

RESULTS

The Architecture of the Palate in Suncus

The sizes of the palates varied in lateral width and anteroposterior length between male and female *Suncus*. However, only male samples, approximately 15.0 mm in mesio-distal length (lateral width of incisors, 1.7 mm; canines, 2.2 mm; premolars, 2.4 mm; and molars, 3.6 mm), were used in this study.

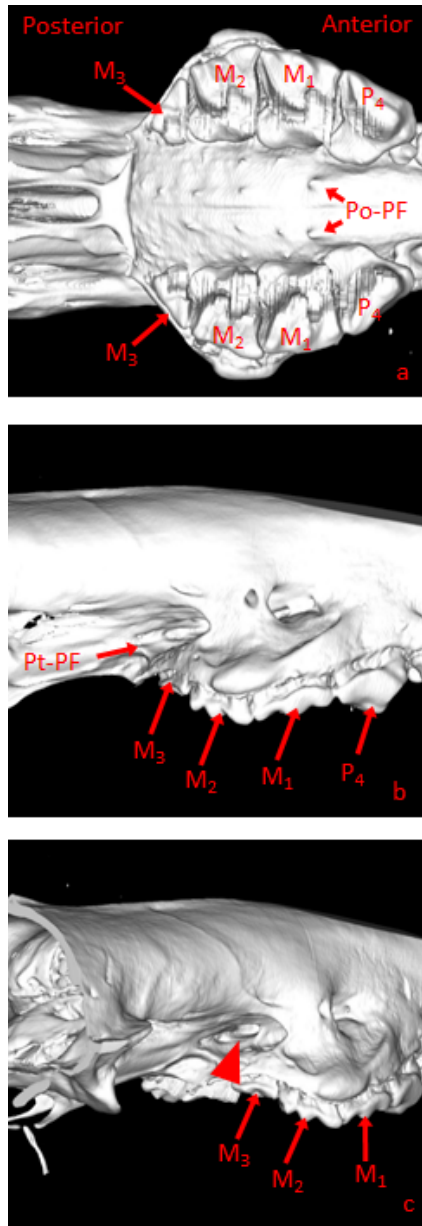


Fig. 2. Three-dimensional reconstruction image of the cranial bone. a) Palatal side. b) Lateral side. c) Oblique direction. A matched pair of posterior palatine foramina was found near the fourth premolar or the first molar. The posterior palatine canal opened at the pterygopalatine fossa situated at the posterior part of the palate. P4: fourth premolar, M1: first molar, M2: second molar, M3: third molar, Po-PF: posterior palatine foramen, Pt-PF: pterygopalatine fossa, ►: opening of posterior palatine canal

The incisive papilla was located between the first incisors, and 12 transverse palatine folds (Fig. 1) were observed immediately posterior to it. The thickness of the mucosal tissue, except for the transverse palatine folds, was found to decrease from approximately 640 μm at the incisal region to 450 μm around the canines to 400 μm near the premolars and 260 μm in the posterior regions.

Multiple holes were found on the oral side of the palatine bone. The distance between the left and right side was measured and the communication was examined. A matched pair of incisive foramina was located near the second incisor (approximately 250 μm in diameter). A matched pair of posterior palatine foramina (approximately 240 μm in diameter) was also found near the fourth premolar or the first molar (Fig. 2a, Fig. 3c). The posterior palatine canal, which opened in the palate as the posterior palatine foramen, extended postero-laterally and connected with the pterygopalatine fossa positioned at the posterior part of the palate (Figs. 2-4). The diameter of the posterior palatine canal was approximately 220 μm near the posterior palatine foramen, 290 μm immediately before communicating with the pterygopalatine fossa, and 250 μm midway between the two. The diameter of the posterior palatine canal was increased as it approached the pterygopalatine fossa. Vessels and nerves were distributed haphazardly within the posterior palatine canal. Arteries were located at the center of the canal, whereas the veins and nerves appeared to change directions from medial to superior to lateral while wrapping around the arteries during their course. Two foramina located near the second and third molars were identified as the greater palatine foramen (approximately 150 μm in diameter) and the lesser palatine foramen (approximately 130 μm in diameter), respectively (Fig. 5a). The greater palatine canal connected with the posterior palatine canal (Fig. 5b), whereas the lesser palatine canal joined the posterior palatine canal near its opening adjacent to the pterygopalatine fossa

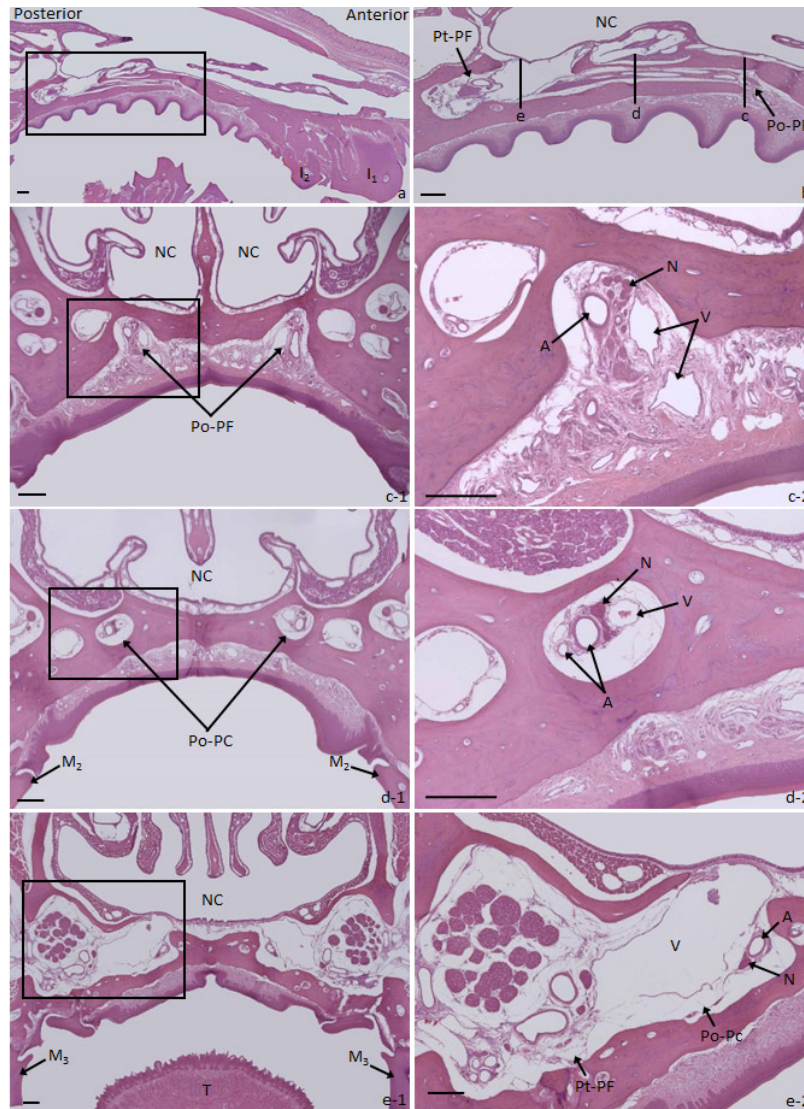


Fig. 3. H-E stained image of the head. a) Sagittal section. b) Magnified image of the square in Fig. 3a. c-1) Frontal section of b. c-2) Magnified image of the square in Fig. c-1. d-1) Frontal section of b. d-2) Magnified image of the square in Fig. d-1. e-1) Frontal section of b. e-2) Magnified image of the square in Fig. e-1. The posterior palatine canal opened into the posterior palatine foramen posteriorly and communicated with the pterygopalatine fossa. I1: first incisor, I2: second incisor, A: artery V: vein, N: nerve, Po-PC: posterior palatine canal, (bar: 200 μ m)

(Fig. 5c). Similar to the posterior palatine fossa and canal, several arteries, veins and nerves were found distributed along the greater and lesser palatine canals.

The Distribution of Lymphatic Vessels in the Palate of the Suncus

The lymphatic vessels in the palate were identified as dark brown canals in 5'-Nase stained serial images (Fig. 6a and b). The vessels were generally flat in shape with very few round canals. Therefore, the diameter had to be calculated from the circumference of the flattened canals.

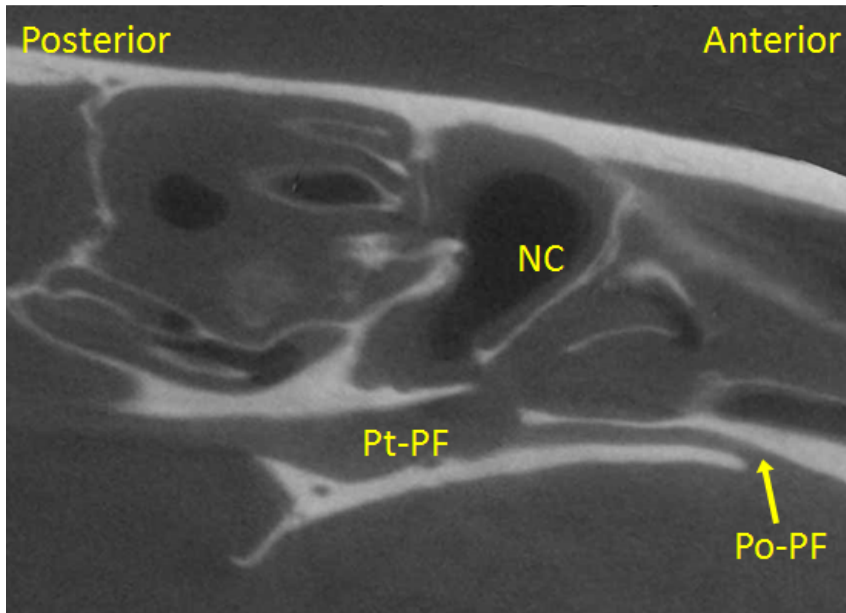


Fig. 4. MPR image showing the distribution of the posterior palatine canal of the cranial bone.

Three-dimensional reconstruction images revealed collecting lymphatic vessels running antero-posteriorly on the periosteum of the bone (Fig. 7). Two thick collecting lymphatic vessels were observed running from the incisive foramen to the posterior palatine foramen on each side and two thin lymphatic vessels ran from the choana to the posterior palatine foramen on both sides of the oral cavity. The diameter of the former increased gradually from approximately 100 μm near the incisive foramen to 120 μm immediately before the posterior palatine foramen, and 110 μm at the middle. Similarly, the diameter of the thin lymphatic vessel was 80 μm near the posterior nares and 100 μm near the posterior palatine foramen, showing an increase in diameter as it ran posteriorly towards the posterior palatine foramen. The thick and thin lymphatic vessels merged at the vicinity of the posterior palatine foramen and entered the posterior palatine foramen. These collecting lymphatic vessels existed bilaterally in the palate, but no connections were noted between the vessels on the left and right sides.

Collecting lymphatic vessels from the palatine mucosa and the alveolus dentalis merged with the collecting lymphatic vessels and coursed along the periosteum of the palate in an antero-posterior direction. The vessels in the palatine mucosa started at the lymphatic capillary immediately below the epithelium (Fig. 6) and subsequently merged with the collecting lymphatic vessels. On the other hand, lymphatic vessels located at the vicinity of the alveolus dentalis were found to be distributed on the periosteum before merging with the lateral branches of the collecting lymphatic vessels anterior to the posterior palatine foramen.

The lymphatic vessels merged near the posterior palatine foramen before entering it and ran along the posterior palatine canals to reach the pterygopalatine fossa. The vessels ran along with arteries, veins and nerves in the posterior palatine canal. The lymphatic vessels entered the posterior palatine foramen from the medial side, wrapped around arteries as they coursed about 30 μm from the bony posterior palatine wall, changed directions from medial to superior to lateral

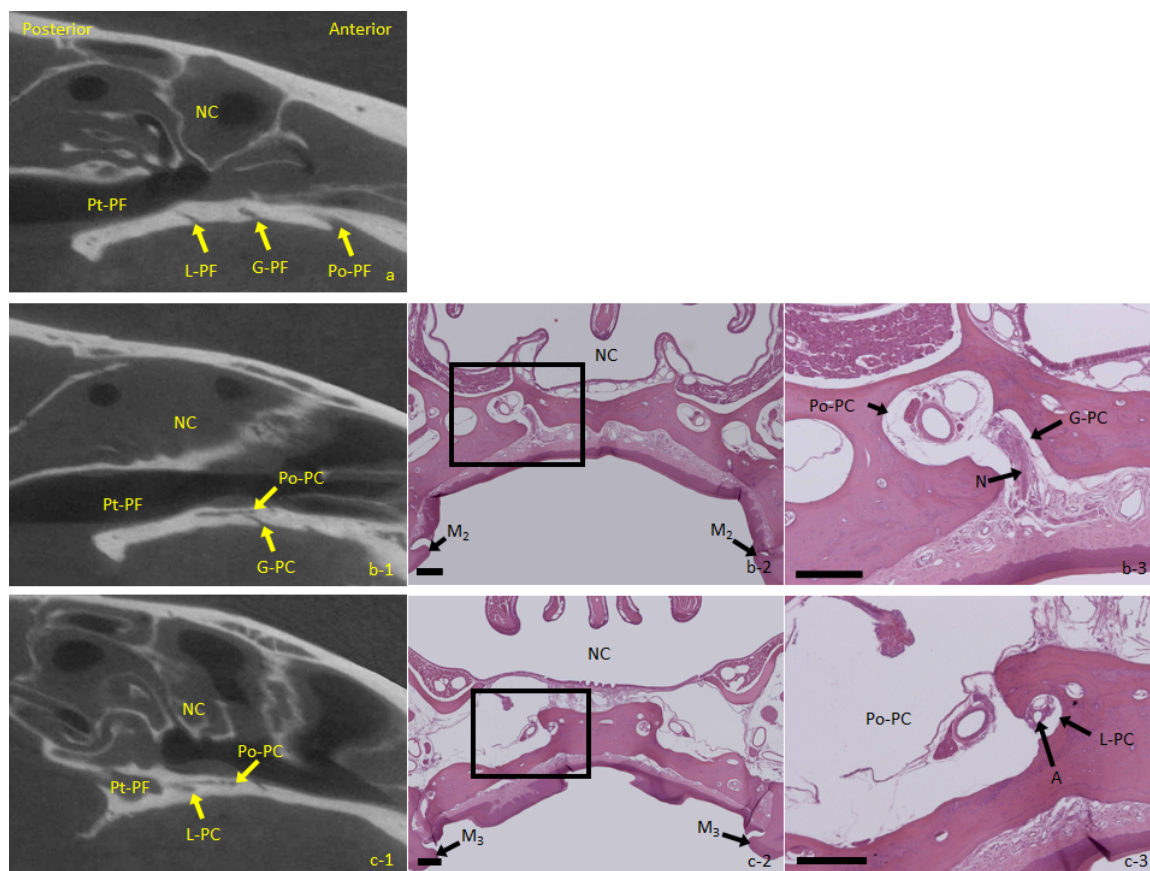


Fig 5. MPR image and H-E stained images showing the distribution of the greater and lesser palatine canals in the cranial bone. a) MPR image of the cranial bone. b-1) MPR images showing the posterior palatine canal merging with the greater palatine canal, and c-1) the lesser palatine canal. b-2) H-E stained sections showing the posterior palatine canal combining with the greater palatine canal. b-3 and c-3) Magnified images of the squares in Figs. b-2 and c-2 (frontal section, bar: 200 μ m). G-PF: greater palatine fossa, L-PF: lesser palatine canal, G-PC: greater palatine fossa, L-PC: lesser palatine canal

until they reached the pterygopalatine fossa (Fig. 8). The diameter of the lymphatic vessels distributed in the posterior palatine canal was approximately 120 μ m near the posterior palatine foramen, 140 μ m near the pterygopalatine fossa, and 130 μ m in the middle. In the posterior palatine canal, the vessels appeared flat in shape, similar to those seen in the palate, before reaching the pterygopalatine fossa.

DISCUSSION

According to Vital Statistics in 2013, the

leading cause of death in Japan was malignant neoplasms resulting in the death of 357,185 people (approximately 30% of the entire mortality) (15). The percentage of oral cancers among the malignant neoplasms was only around 2%; however, unlike in Europe and the US, tracing mortality due to oral cancers has shown an upward trend in Japan (16). Metastasis of oral cancers to the lymph nodes frequently occurs due to failure in early diagnosis, leading to a poor prognosis. Although the occurrence of carcinomas in the hard palate is generally low among the oral cancers (17), it is well known that they tend

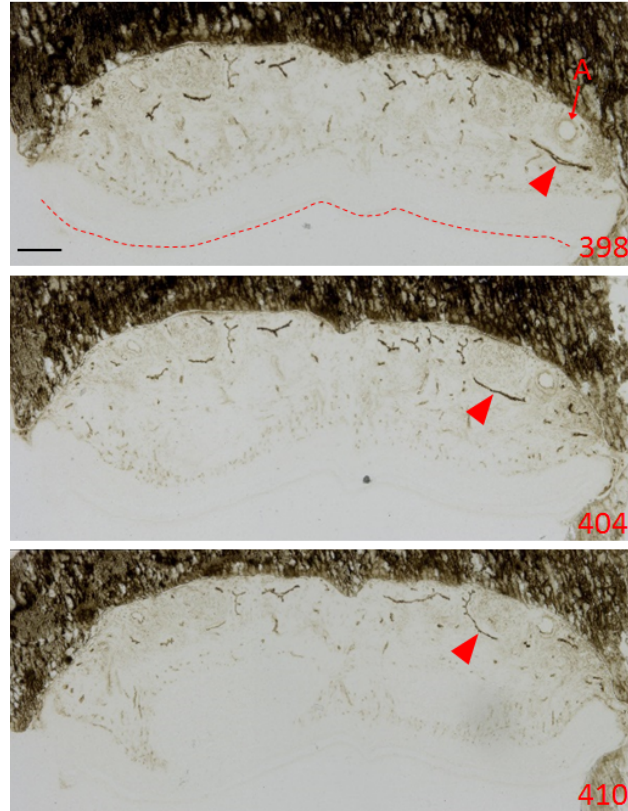


Fig. 6. Lymphatic vessels image stained with 5'-Nase near the third premolar. Image show the anterior (398) to posterior (410) of palate. Lymphatic vessels stained with dark brown were observed. ► : lymphatic vessels from the alveolus dentalis. Dotted line: epithelial layer, (frontal section, bar: 200 μ m)

to cause direct metastasis in the deep lymph nodes, which are the regional lymph nodes for the palate and the maxillary lingual gingiva (18). However, detailed routes of metastases to these nodes have not been elucidated yet. Our research group has been investigating the craniocervical architecture of lymphatic vessels in mammals, including humans (2-11,13,14). The architecture of lymphatic capillaries in the palate has been reported previously (1) but there is no study describing the distribution of collecting lymphatic vessels. Therefore, in the present study, we investigated the architecture and routes of the lymphatic vessels from the palate. Due to difficulties in obtaining human samples, experimental animals were utilized in this study.

Many studies have used rodents such as mice, rats, guinea pigs, and hamsters as experimental animals. It is important to judge whether the results obtained from the selected experimental animal will reflect humans. The various responses obtained from experimental animals are specific to each species and may be different from those in humans. Thus, one of the most important criteria for the selection of an experimental animal is the extent of similarity it has to humans in terms of both morphology and physiology. It is essential to select an animal that has similar anatomical features to humans in morphological studies, such as the present one. Recently, *Suncus*, classified as Insectivora Soricidae Crocidurinae *Suncus*, are gaining popularity for use as a small

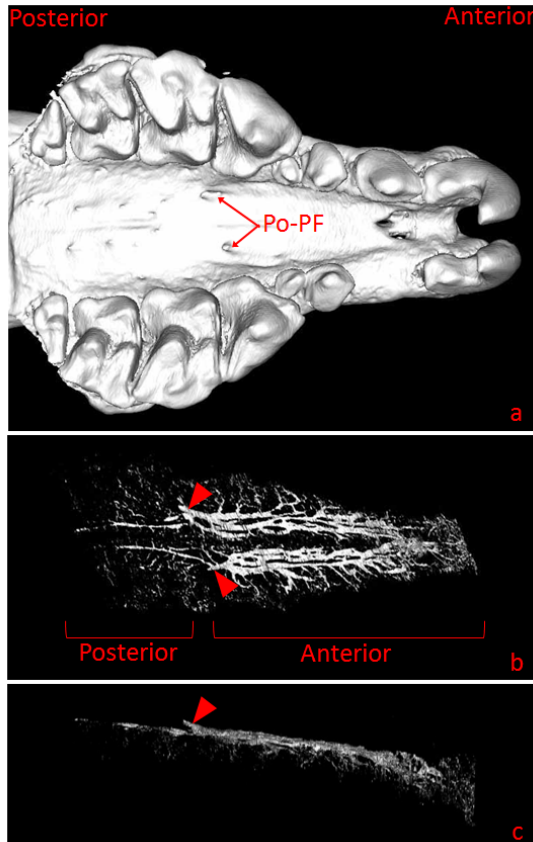


Fig. 7. Reconstruction image. *a)* Three-dimensional image of the cranial bone by Micro CT (from the palatal side). *b)* Three-dimensional image of lymphatic vessels by the serial section (from the palatal side). *c)* Three-dimensional image of lymphatic vessels by the serial section (from the lateral side). The thick lymphatic vessels from the anterior and thin lymphatic vessels from the posterior merged at the vicinity of the posterior palatine foramen and entered the posterior palatine foramen. ► : Collecting lymphatic vessels entering the posterior palatine foramen

experimental animal. They were first considered for use in experimental studies in 1972 (19,20). In recent years, they have been used in several medical studies including emetic responses (21-25), tonsils (26-30), fatty liver in lifestyle diseases (31-35), and also in dental research (36-40). Since its emergence as an ancestor of placental mammals during the Cretaceous period, various species including primates have been differentiated

from the order Insectivora. However, species from this order have been known to maintain the primitive phenotypes of placental mammals (41). One of the most prominent characteristics of the oral cavity in this species is that they have all types of teeth. The dental formula of mice or rats ($I1/1C0/0P0/0M3/3 = 16$) is largely different from that of a typical mammal ($I3/3C1/1P4/4M3/3 = 44$); the former present with edentulous areas due to missing canines and premolars. On the other hand, *Suncus* possess a similar dental formula ($I3/1C1/1P2/1M3/3 = 30$) to that of a typical mammal. In addition, it is known that tooth buds of primary teeth are temporarily developed during the embryonic stage in *Suncus* (42). These facts indicate that they have certain basic characteristics similar to those seen in mammals such as heterodonty and diphyodonty. Since jaw bone morphology is affected by the form and number of teeth, the oral anatomy of *Suncus* with heterodonty and diphyodonty is considered to be closer to humans relative to the rodents. The distribution of lymphatic vessels is affected by the morphology of the hard tissue. Therefore, since the *Suncus* exhibits a jaw bone morphology similar to that of humans, we considered it to be a suitable for use as an experimental animal in the present study.

Comparison between the morphology of the palate in Suncus and humans

In the present study, we found several differences in the structure of the palate between humans and *Suncus*. In humans, the greater palatine canal connects the palate and the pterygopalatine fossa forming a route for the greater palatine nerve and the descending palatine artery, which gives out branches that descend into the lesser palatine canals in the palatine bone. In contrast, in *Suncus*, the posterior palatine canal was found to connect the palate and the pterygopalatine fossa; both greater and lesser palatine canals were merged with the

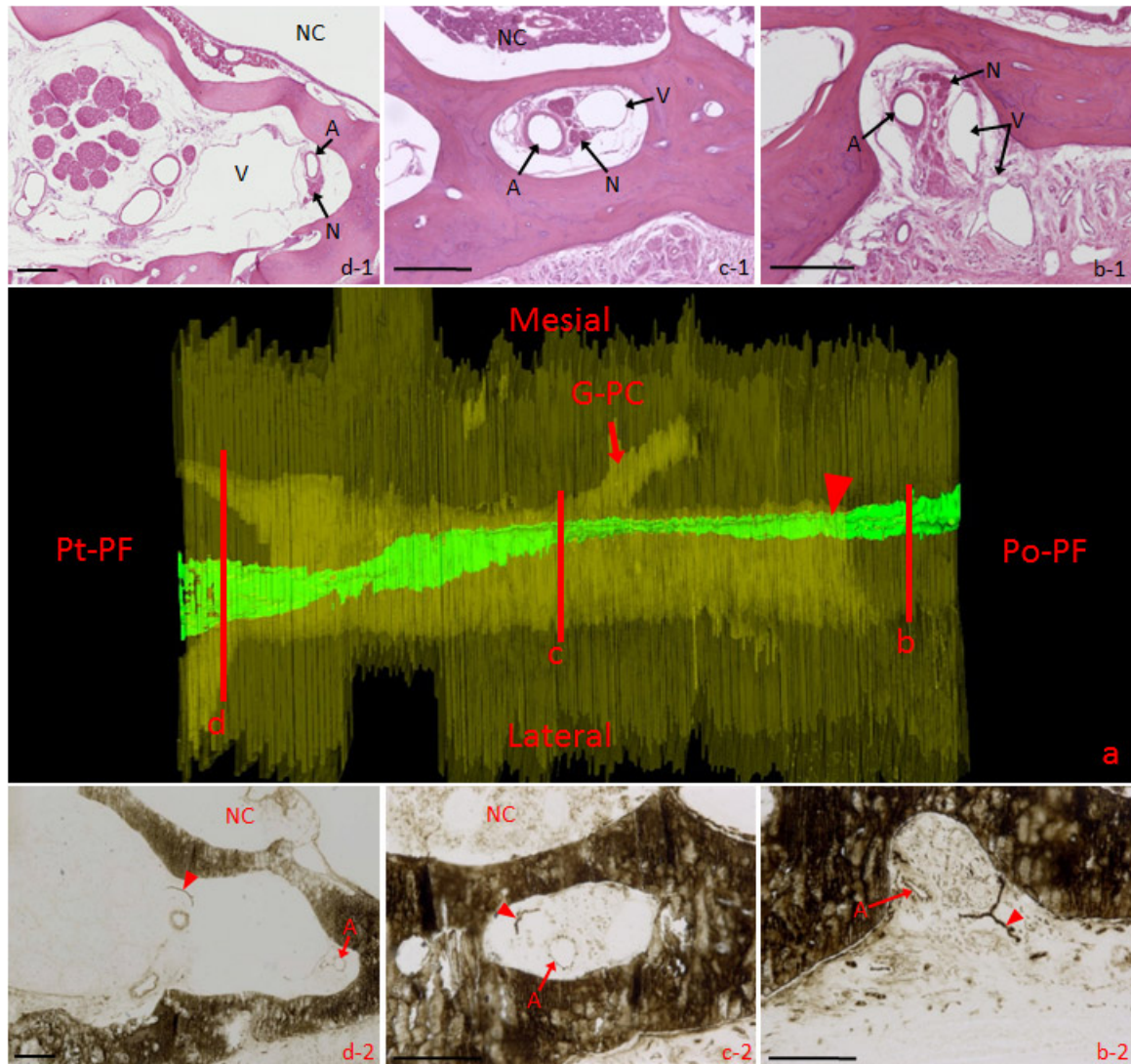


Fig. 8. Reconstruction image of lymphatic vessels in the posterior palatine canal. a) Overlapped three-dimensional reconstruction image of lymphatic vessels in the posterior palatine canal and surrounding tissue. b-1) H-E stained image of area b from Fig. a. b-2) 5'-Nase stained image of area b in Fig. a (frontal section; bar: 200 &μm). c-1) H-E stained image of area c in Fig. a. c-2) 5'-Nase stained image of area c in Fig. a. d-1) H-E stained image of area d in Fig. a. d-2) 5'-Nase stained image of area d in Fig. a. The lymphatic vessels medially entered the posterior palatine foramen and ran towards the pterygopalatine fossa changing the direction gradually to the lateral side. ► : lymphatic vessel

posterior palatine canal based on our observations of the Micro CT and tissue sections. The role of the greater palatine canal (in humans) and posterior palatine canal (in *Suncus*) is the same in terms of connecting the palate with the pterygopalatine fossa.

Joints within the bone in the palate are recognized as sutures, and it is known that synostosis progresses with age in humans. In contrast, synostosis of the palatine process of the maxilla commences during the embryonic stage in the *Suncus* and is completed during

the early stages after birth (19,20). Since the Suncus used in the present study were 4-week-old adults, the joints in the maxillary and palatine bones were completely fused, and the components of the posterior palatine foramen and the posterior palatine canal were not elucidated.

In humans, the greater and lesser palatine foramina, which open into the pterygopalatine fossa, are located distal to the second molars in the posterior part of the palate. On the other hand, in the Suncus, the posterior palatine foramen was located near the fourth premolar or the first molar, while the greater and lesser palatine foramina were located adjacent to the second and third molars. The posterior palatine foramen was situated in the middle of the palate, indicating the presence of an additional route to the pterygopalatine fossa in the Suncus. This may be attributed to the fact that the antero-posterior length and lateral width of the palate in Suncus is greater than that of humans. In the present study, arteries, veins, nerves, and lymphatic vessels were observed inside the posterior palatine canal. Since the antero-posterior length is relatively high in Suncus, the collection and delivery of blood and lymph to and from the anterior or posterior region is not very effective. Thus, it is thought that the posterior palatine canal is present at the center of the palate and serves as one of the routes to the pterygopalatine fossa.

In the posterior palatine canal, the arteries were located in the middle, whereas the veins and nerves ran posterior to and around the arteries, changing directions from medial to superior to lateral. These findings indicate the importance of the positional relationship between the maxillary artery that branches into the descending palatine artery and is distributed in the palate, and the maxillary vein that collects the venous blood from the palate. Since the maxillary artery is more medially located than the maxillary vein, the position of these vessels must have changed in the posterior palatine canal in

order to facilitate the transfer of fluids between them.

The relation between distribution of lymphatic vessels and the surrounding tissue

Lymphatic vessels in Suncus were flatter than those in humans; very few round-shaped canals were observed. This could be due to the strong attachment of the underlying connective tissue to the bone resulting in the flattening of the vessels.

Two thick collecting lymphatic vessels ran bilaterally in the palate from the incisive foramen to the posterior palatine foramen; in addition, thin lymphatic vessels were also observed running from the choana to the posterior palatine foramen. The lymph vessel from the alveolus dentalis merged with the lateral collecting vessel indicating that the lateral branch of the collecting lymphatic vessel collects lymph from the lateral area of the palate, whereas the medial branch of the collecting lymphatic vessel collects lymph from the medial area of the palate. Additionally, it was confirmed that the thin collecting lymphatic vessels ran antero-posteriorly from the choana to the posterior palatine foramen, where fewer and thinner lymphatic vessels were observed when compared with the region anterior to the posterior palatine foramen. Because synostosis of transverse palatine suture occurs during the embryonic stage in the Suncus, we could not discriminate the posterior palatine foramen, greater and lesser palatine foramina (19,20). However, we postulated that the posterior palatine foramen is a substitute for the greater palatine foramina in humans because a relatively thick nerve runs in the posterior palatine canal. This was explained by the fact that the greater and lesser palatine foramina opened posteriorly to the posterior palatine foramen, and the lymphatic vessels in this region coursed towards the pterygopalatine fossa through these foramina, preventing the development of collecting lymphatic vessels. No connection between the left and right collecting vessels

was found beyond the midline, indicating the existence of a “watershed” in the palate.

The collecting lymphatic vessels on the periosteum entered the posterior palatine foramen and coursed towards the pterygopalatine fossa through the posterior palatine canal. The thickness of the lymphatic vessels increased as they approached the posterior palatine foramen. Taken together, these findings suggest that in the palate, the lymph flows into the posterior palatine foramen and the pterygopalatine fossa via the posterior palatine canal. Thereafter, it flows into the deep cervical lymph nodes. The lymphatic vessels along with veins and nerves enter the posterior palatine foramen into the pterygopalatine fossa, changing positional relationship with the arteries from medial to superior to lateral directions; thereafter, the vessels stay in position between the bony walls and the arteries until they reach the pterygopalatine fossa. The reason for the change in direction to the lateral side of the lymphatic vessels could be explained by the necessity to flow into the deep cervical lymph nodes along with the internal jugular vein, which also changes its direction. The positioning of the lymphatic vessels between the walls of the bone and the arteries could be attributed to the function of lymphatic transport; however, this could not be elucidated clearly in the present study.

The pterygopalatine fossa is located immediately behind the palate in *Suncus*, where the lymph fluid drains horizontally towards the posterior regions. On the other hand, in humans the pterygopalatine fossa is located superiorly; this feature contradicts common sense as lymphatic vessels are not capable of flowing against gravity. In humans, the face is bent at a right angle to the axis of the body owing to erect bipedalism, which could account for the elevated position of the pterygopalatine fossa relative to the palate. Although the lymphatic flow from the palate is not very effective, it reached the pterygopalatine fossa, which is located higher than the palate. Then, the fluid drained into the

deep cervical lymph node by flowing via the lateral cervical region, without passing through the submandibular lymph node. Some parts of the distribution of lymphatic vessels in this study seem to contradict flowing mechanisms; however, considering the evolution process could help us understand the reasons for the anatomical distributions of lymphatic vessels.

ACKNOWLEDGMENTS

We would like to express our deep appreciation to Professor Sen-ichi Oda and Lecturer Takamichi Jogahara (Okayama University of Science, College of Science, Department of Zoology) for donating the *Suncus* for this study. Moreover, we are grateful to faculty and staff members of the Institute for Experimental Animal Sciences of the Iwate Medical University, the Department of Oral Health Science Division of Orthodontics and the Department of Anatomy Division of Functional Morphology for their assistance and cooperation. The abstract of this study was presented at the 74th Annual Meeting of the Japanese Orthodontic Society (2015, Fukuoka).

CONFLICT OF INTEREST AND DISCLOSURE

All authors declare that no competing financial interests exist.

REFERENCES

1. Fujimura, A, Y Sato, M Shoji, et al: Lymphatic architecture of the oral region- Palatum-. *Dent. Jpn.* 43 (2007), 7-11.
2. Fujimura, A, Y Nozaka: Analysis of the three-dimensional lymphatic architecture of the periodontal tissue using a new 3D reconstruction method. *Microsc. Res. Tech.* 56 (2002), 60-65.
3. Fujimura, A, S Seki, M-Y Liao, et al: Three dimensional architecture of lymphatic vessels in the tongue. *Lymphology* 36 (2003), 120-127.
4. Sato, Y, A Fujimura: Lymphatic architecture and distribution beneath the buccal mucosa. *Dent. J. Iwate Med. Univ.* 34 (2009), 7-17.

5. Fujimura, A, M Masuyama: Lymphatic distribution in the mouse periodontal ligament. *Microvasc. Rev. Commun.* 3 (2009), 2-10.
6. Liang, J-C, A Fujimura: Lymphatic architecture beneath the mucosal membrane of the tongue. *Iwate Med. Univ.* 25 (2000), 283-291.
7. Fujimura, A, Y Sato, M Shoji, et al: Lymphatic architecture of the oral region:- beneath the buccal mucosa. *Microvasc. Rev. Commun.* 1 (2007), 9-11.
8. Liao, M-Y, A Fujimura: The distribution of lymphatic vessels in gingiva. *Microvasc. Rev. Commun.* 2 (2009), 2-7.
9. Masuyama, M, A Fujimura: Lymphatic distribution in the mouse periodontal ligament. *Microvasc. Rev. Commun.* 3 (2009), 2-10.
10. Seki, S, A Fujimura: Three-dimensional changes in lymphatic architecture around VX2 tongue cancer—dynamic changes after administration of antiangiogenic agent. *Lymphology* 36 (2003), 199-208.
11. Zhang, B, M Miura, RC Ji, et al: Structural organization and fine distribution of lymphatic vessels in periodontal tissues of the rat and monkey: A histochemical study. *Okajimas Folia Anat. Jpn.* 77 (2000), 93-107.
12. Kawamoto, T, M Shimizu: A method for preparing 2- to 50-micron-thick fresh-frozen sections of large samples and undecalcified hard tissues. *Histochem. Cell Biol.* 113 (2000), 331-339.
13. Ando, Y, O Murai, Y Kuwajima, et al: Lymphatic architecture of the human gingival interdental papilla. *Lymphology* 44 (2011), 146-154.
14. Ando, Y, A Fujimura: Lymphatic architecture of human periodontal tissue beneath the oral epithelium of the free gingiva. *Microvasc. Rev. Commun.* 3 (2009), 17- 24.
15. Outline of Vital Statistics in Japan, 2011. Ministry of Health, Labour and Welfare. <http://www.mhlw.go.jp/toukei/saikin/hw/jinkou/geppo/nengai11/kekka03.html>, (2015-12-10)
16. Tanaka, S, T Sobue: Comparison of oral and pharyngeal cancer mortality in five countries: France, Italy, Japan, UK and USA from WHO mortality database (1960-2000). *Jpn. J. Clin. Oncol.* 35 (2005), 488-491.
17. Report of head and neck cancer registry of Japan, Clinical statistics of registered patients, 2002. Oral cavity. *Jpn. J. Head and Neck Cancer* 32 (2006), 15-34.
18. Földi, M, E Földi (Eds): *Lehrbuch Lymphologie für Ärzte, Physiotherapeuten und Masseur/med*, Bademeister. München. Elsevier GmbH. 1989, pp. 30-51.
19. Kondo, K, S Oda, J. Kitoh, et al: *Suncus Murinus Biology of the Laboratory Shrew*. JSSP. 1985, pp. 189-193.
20. Oda, S, K Tohya, T Miyaki: *Biology of Suncus*. JSSP. 2011, pp. 3-8.
21. Mine, Y, S Oku, N Yoshida: Anti-emetic effect of mosapride citrate hydrate, a 5-HT₄ receptor agonist, on selective serotonin reuptake inhibitors (SSRIs)-induced emesis in experimental animals. *J. Pharmacol. Sci.* 121 (2013), 58-66.
22. Yamamoto, K, SW Chan, JA Rudd, et al: Involvement of hypothalamic glutamate in cisplatin-induced emesis in *Suncus murinus* (House Musk Shrew). *J. Pharmacol. Sci.* 109 (2009), 631-634.
23. Kaji, T, H Saito, S Ueno, et al: Comparison of various motion stimuli on motion sickness and acquisition of adaptation in *Suncus murinus*. *Jikken Dobutsu.* 39 (1990), 75-79.
24. Ito, H, M Nishibayashi, S Maeda, et al: Emetic responses and neural activity in young musk shrews during the breast-feeding/weaning period: Comparison between the high and low emetic response strains using a shaking stimulus. *Exp. Anim.* 54 (2005), 301-307.
25. Horikoshi, K, T Yokoyama, N Kishibayashi, et al: Possible involvement of 5-HT₄ receptors, in addition to 5-HT₃ receptors, in the emesis induced by high-dose cisplatin in *Suncus murinus*. *Jpn. J. Pharmacol.* 85 (2001), 70-74.
26. Doi, A, M Okano, H Akagi, et al: Blood vascular architecture of the palatine tonsil in the musk shrew (*Suncus murinus*): Scanning electron microscopic study of corrosion casts. *Anat. Sci. Int.* 78 (2003), 62-67.
27. Sakai, K, H Imada, M Shinzato, et al: Peculiar tonsil-like structure near vagina of the laboratory shrew, *Suncus murinus*. *Okajimas Folia Anat. Jpn.* 89 (2013), 105-112.
28. Sakai, K, G Isomura: Fine structure of the anal tonsillar epithelium in the laboratory shrew (*Suncus murinus*). *Okajimas Folia Anat. Jpn.* 81 (2004), 25-32.
29. Sakai, K, A Tanaka, G Isomura: Developmental study of the anal tonsil in the laboratory shrew, *Suncus murinus*. *Arch. Histol. Cytol.* 65 (2002), 97-108.
30. Tohya, K, M Kimura: High endothelial venule and lymphocyte homing of the musk shrew palatine tonsil. *Kaibogaku Zasshi.* 69 (1994), 661-668.
31. Nagayoshi, A, N Matsuki, H Saito, et al: Role of acyl coenzyme A cholesterol acyltransferase in intrahepatic processing of apo B-lipoprotein in *suncus*. *J. Biochem.* 118 (1995), 259-264.
32. Liang, YQ, M Kinoshita, T Muto, et al: Defect in an intrahepatic degradation of

- apolipoprotein B in suncus: An animal model of hypobetalipoproteinemia. *J. Biochem.* 123 (1998), 28-32.
33. Nagayoshi, A, N Matsuki, H Saito, et al: Defect in assembly process of very-low-density lipoprotein in suncus liver: An animal model of fatty liver. *J. Biochem.* 117 (1995), 787-793.
 34. Yasuhara, M, T Ohama, N Matsuki, et al: Induction of fatty liver by fasting in suncus. *J. Lipid Res.* 32 (1991), 887-891.
 35. Yasuhara, M, T Ohama, N Matsuki, et al: Deficiency of apolipoprotein B synthesis in *Suncus murinus*. *J. Biochem.* 110 (1991), 751-755.
 36. Koike, Y: development of the subpulpal wall in the lower molars of *Suncus murinus* (soricidae, insectivora). *Aichi Gakuin. J. Dent. Sci.* 36 (1998), 221-226.
 37. Miyado, M, H Ogi, G Yamada, et al: Sonic hedgehog expression during early tooth development in *Suncus murinus*. *Biochem. Biophys. Res. Commun.* 363 (2007), 269-275.
 38. Yamanaka, A, H Iwai, M Uemura, et al: Patterning of mammalian heterodont dentition within the upper and lower jaws. *Evol. Dev.* 17 (2015), 127-138.
 39. Takayanagi, T: Histological change and apoptosis in the lower molars of *Suncus murinus* (Insectivora). *Aichi Gakuin. J.* 42 (2004), 37-49.
 40. Kondo, S: Morphological study on the development of cheek tooth germs in the *Suncus murinus* fetus (Soricidae, Insectivora). *Aichi Gakuin. J.* 23 (1985), 697-730.
 41. Barnard, CJ: *The Encyclopaedia of Animals*. Macdonald, DW (Ed.), London. Equinox Ltd., London (2000), 26-31.
 42. Sasaki, C, T Sato, Y Kozawa: Apoptosis in regressive deciduous tooth germs of *Suncus murinus* evaluated by the TUNEL method and electron microscopy. *Arch. Oral Biol.* 46 (2001), 649-660.

Akira Fujimura, DDS, PhD
Department of Anatomy, Division of
Functional Morphology
Iwate Medical University, Japan
2-1-1 Nishitokuta
Yahaba-Cho, Shiwa-Gun
Iwate 028-3694, Japan
TEL: +81-19-651-5111(ex.5842)
FAX: +81-19-908-8010
E-mail: akifuji@iwate-med.ac.jp